



Noninvasive Monitoring and Evaluation of the Renal Structure and Function in a Mouse Model of Unilateral Ureteral Occlusion Using Microcomputed Tomography

Jiangang Hou^{1,2}, Masayuki Fujino^{1,3}, Songjie Cai¹, Qiang Ding², Xiao-Kang Li¹

¹*Division of Transplantation Immunology, National Research Institute for Child Health and Development, Tokyo, Japan*

²*Department of Urology, Huashan Hospital, Fudan University, Shanghai, China*

³*AIDS Research Center, National Institute of Infectious Diseases, Tokyo, Japan*

Mouse unilateral ureteral occlusion (UUO) is widely used as a model of renal experimental obstructive nephropathy with interstitial fibrosis. Microcomputed tomography (micro-CT) imaging has the potential to produce quantitative images. The aim of this study was to establish standard images of micro-CT for renal anatomic and functional evaluations in a mouse model of UUO. UUO was induced in adult male mice BALB/c. In total, 27 mice were used in this study. Three mice per group (a total of 6 groups) were examined with contrast-enhanced micro-CT prior to UUO (day 0) and on days 1, 3, 5, 7, 10, and 14 after UUO. In order to determine the histopathologic correlations at each point in time, contrast-enhanced micro-CT imaging was performed in the 18 remaining mice. All animals were sacrificed, and both kidneys were harvested after the final micro-CT examination. UUO resulted in hydronephrosis and changes in the renal parenchyma. The predominant alteration was substantial changes in the hemodynamics of the renal vascular system after ureteral obstruction for 24 hours or longer, which may be resulting from increased action of vasoconstrictors versus vasodilators. The renal parenchyma was significantly reduced after 1 week, and the features of the histologic changes supported the findings of the micro-CT images. In the contralateral unobstructed kidneys, the images showed a normal structure and function and the pathohistology

Corresponding author: Xiao-Kang Li, MD, PhD, Division of Transplantation Immunology, National Research Institute for Child Health and Development, 2-10-1 Okura, Setagaya-ku, Tokyo, 157-8535 Japan.
Tel.: +81 3 3416 0181; Fax: +81 3 3417 2864; E-mail: ri-k@ncchd.go.jp

revealed a normal histoarchitecture. Micro-CT is a useful tool for providing noninvasive monitoring and evaluating the renal structure and function.

Key words: Noninvasive monitoring – Unilateral ureteral occlusion – Microcomputed tomography

In renal disease, a number of diseases involve structural changes and functional abnormalities. Most forms of chronic kidney disease tend to result in progressive loss of the renal function due to the effects of glomerular sclerosis and or interstitial fibrosis. Approximately 80% of the total kidney volume is composed of tubular epithelial cells and cells within the interstitial space. Unilateral ureteric obstruction (UUO) is a widely used model of experimental renal hydronephrosis, inflammation, and fibrosis.¹ However, simultaneous studies of structural changes and functional abnormalities require proper methods.

X-ray computed tomography (CT), which exhibits proven diagnostic performance in the clinical setting, was recently redeveloped as an experimental tool for obtaining long-term morphologic observations in rats and mice, with the ability to rapidly acquire high-quality images. Micro-CT is already an established technology for imaging diverse mineralized animal tissues and, with enhancement contrast, provides sufficient intra-organ contrast to detect soft organs.²

The research goal of this study was to evaluate the efficacy of the micro-CT technique for detecting and monitoring the renal structure and function in a murine UUO model.

Materials and Methods

Animals

Male BALB/c mice weighing 20 to 25 g were purchased from Shizuoka Laboratory Animal Center (Shizuoka, Japan). The mice were housed at 5 animals or fewer per cage in a limited access area, with a room temperature of $20 \pm 1^\circ\text{C}$ and humidity of $50 \pm 10\%$ and access to food and tap water, in accordance with the guidelines of the Animal Use and Care Committee of the National Research Institute for Child Health and Development, Tokyo, Japan. All animal experiments were approved by this committee and performed according to its recommendations.

UUO procedure

UUO was performed as previously described.³ Briefly, using a temperature-controlled operating table heated to body temperature, with the animal

anesthetized with isoflurane/oxygen, and a high-quality binocular microscope to visualize the operating field, the right ureter was exposed and permanently ligated twice with 7-0 silk sutures. According to the study protocol, 3 mice were examined with contrast-enhanced micro-CT prior to UUO (day 0) and on days 1, 3, 5, 7, 10, and 14 after UUO. In order to determine the histopathologic correlations at each point in time, contrast-enhanced micro-CT imaging was performed in the 18 remaining mice. All animals were sacrificed, and both kidneys were harvested after the final micro-CT examination.

Micro-CT procedures

The micro-CT device (LCT-200 scanner) was provided by Hitachi Aloka Medical, Ltd (Tokyo, Japan). The micro-CT imaging system included an imaging scanner and controlling computer. All images were reconstructed using the software program provided by Hitachi Aloka Medical, Ltd. The mice were anesthetized with isoflurane/oxygen general anesthesia, and 0.5 mL of radiopaque contrast agent was injected through the tail vein. Image acquisition was started 5 and 30 minutes after contrast agent injection (Fig. 1A–D).

Image and quantitative analysis

In all 21 mice, the renal length and thickness and parenchymal thickness were measured manually using the CTAN software package (SkyScan, Aartselaar, Belgium) (Fig. 1E and F). The renal engorgement/excretion time was measured after contrast agent injection corresponding to a 3-dimensional model of the kidneys (Fig. 1E' and F').

Histopathology and light microscopy

After the micro-CT examinations, the kidneys were removed and fixed in buffered 10% formalin, embedded in paraffin wax, and sectioned into 5- μm -thick coronal slices, as described elsewhere.⁴ A coronal slice was selected at the middle level on the anterior-posterior axis, which corresponded to the CT imaging

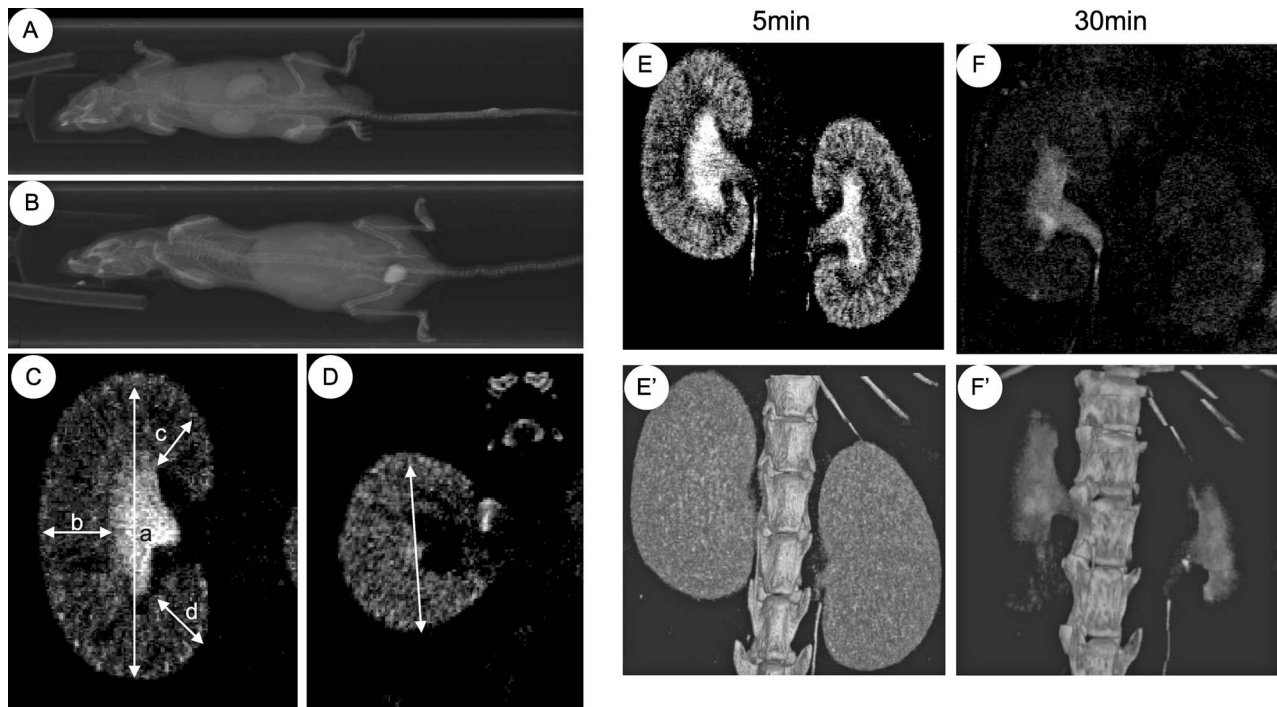


Fig. 1 Imaging of the mouse kidney. Image acquisition was started 5 (A) and 30 (B) minutes after radiopaque contrast agent injection. (C) A coronal slice shows the renal length (a) and parenchymal thickness (b, c, d). (D) An axial slice shows the renal thickness in a BALB/c mouse. (E and F) *In vivo* coronal images of male BALB/c mice using contrast agent and (E' and F') 3-dimensional models of the kidneys and bone. The images were acquired at 5 (E and E') and 30 (F and F') minutes after injection of the contrast agent.

slab, and the sections were subsequently stained with hematoxylin-eosin, as previously described.⁵

Statistical analysis

All values are reported as the mean \pm SD. The statistical analyses were performed using Student's *t*-test, and the results were considered to be statistically significant at a *P* value of < 0.05 .

Results

Anatomical findings

As shown in Fig. 2, the images revealed structural changes in the kidney tissue after UUO. The absolute renal coronal length, parenchymal thickness and axial renal thickness were measured in all kidneys. The renal parenchymal thickness was found to be severely reduced 1 week after UUO. Two weeks later, the renal parenchyma remained a thin wall, with no function (Fig. 2A). The renal coronal parenchymal thickness was found to decrease over time on the UUO side, whereas there were no marked changes on the contralateral side. Significant differences were observed in the changes

in the renal parenchymal thickness between the 2 sides on days 7 ($P < 0.05$) and 14 ($P < 0.01$). The mean thickness of the renal parenchyma on the UUO side rapidly decreased after UUO, from 6.3 ± 1.1 cm on day 0 to 2.5 ± 1.1 cm on day 7. However, no marked changes were observed in the renal coronal length or axial thickness (Fig. 2B).

Functional results

The contrast-enhanced micro-CT images displayed a normal structure and function of the kidneys prior to UUO (Fig. 3). The length and thickness of the right and left kidney were similar with no significant differences. After 30 minutes, the contrast agent was excreted from the kidneys. Figure 3 shows the findings obtained 1 day after UUO, at which time the contralateral unobstructed kidney (CUK) exhibited a normal structure and function, whereas UUO resulted in hydronephrosis, although there were no changes in the length or thickness of the renal parenchyma. Renal engorgement was initially delayed, after which the contrast agent was slowly evacuated after 30 minutes. In contrast, the histoarchitecture showed no visible pathologic

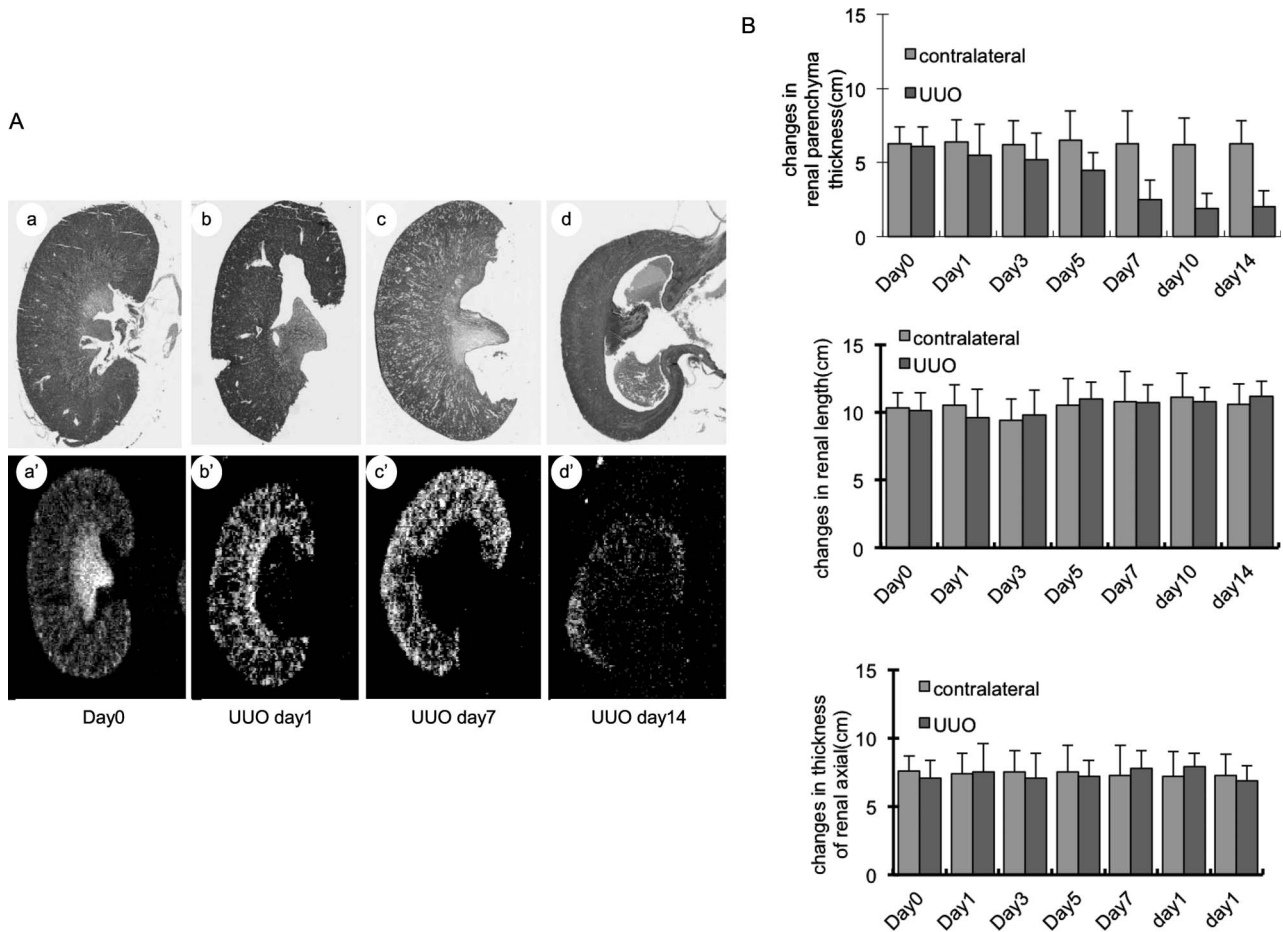


Fig. 2 Structural changes in the kidney after UO. (A) Changes in the renal parenchymal thickness after UO. The images showed that the renal parenchymal thickness was severely reduced 1 week after UO. Two weeks later, the renal parenchyma remained a thin wall, with no function. (B) The graph illustrates the changes in the renal coronal length, parenchymal thickness, and axial renal thickness. The renal coronal parenchymal thickness was found to decrease over time on the UO side, whereas it remained consistent on the contralateral side. In contrast, the renal coronal length and axial thickness demonstrated no changes.

changes (Fig. 4). However, 1 week later, the UO side demonstrated severe hydronephrosis, with thinner parenchyma, than the contralateral side. Although the contrast agent had accumulated in the tissue, the right kidney continued to display a reduced function. After 2 weeks, the UO side displayed extremely severe hydronephrosis, whereas the parietes of the renal parenchyma remained intact. The right kidney exhibited no engorgement or excretion (Fig. 3).

Histological results

Hematoxylin-eosin staining revealed progressive tubular injury on the UO side (Fig. 4). One day after UO, there were no visible pathologic changes. In contrast, abnormal changes, such as morpho-

logic changes manifested by proximal tubule dilation, tubular atrophy, and extracellular matrix (ECM) accumulation, were evident on day 7. After 2 weeks, light micrographs of the kidney cortex showed tubular atrophy, tubules with collapsed and dilated lumina, and increased interstitial spaces with mononuclear and interstitial cells.

Discussion

The current study describes an approach that enables simultaneous anatomic and functional information as well as rigorous histopathologic correlations to be obtained using contrast-enhanced micro-CT as a single diagnostic test in a mouse model of UO.

Animal models of UO have been refined to elucidate the pathogenesis of obstructive nephrop-

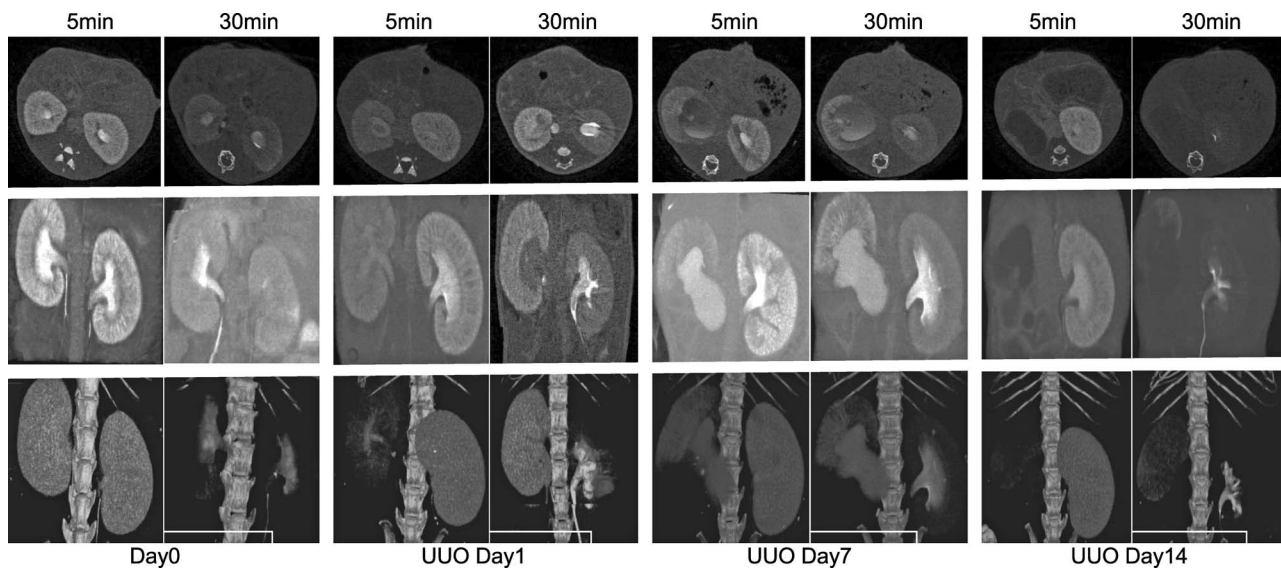


Fig. 3 Images of the structure and function of the kidneys before and on days 1, 7, and 14 after UUO. Before UUO, the renal length and thickness of the right and left kidneys were same. After 30 minutes, the contrast agent was excreted from the kidneys. One day after UUO, the contralateral unobstructed kidney displayed a normal structure and function. The UUO induced hydronephrosis, although the length and thickness of the renal parenchyma did not change. Renal engorgement was initially delayed, after which the contrast agent was slowly evacuated after 30 minutes. Seven days later, the UUO had induced severe hydronephrosis, and the parenchyma was thinner than normal. Although the contrast agent had accumulated in the tissue, the kidney continued to display a reduced function. After 14 days, the UUO side demonstrated extremely severe hydronephrosis, although and the parietes of the renal parenchyma remained intact. The right kidney exhibited no engorgement or excretion.

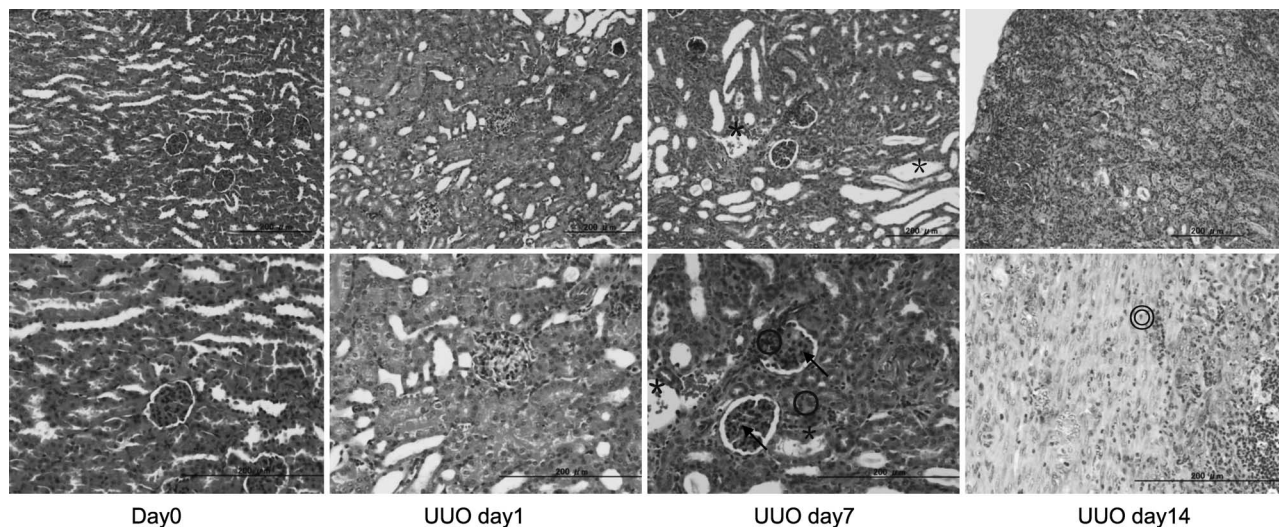


Fig. 4 Morphologic changes in the renal cortex before and on days 1, 7, and 14 after UUO. Before UUO, the renal displayed a normal structure, with a histoarchitecture with a distinct cortex, medulla, and renal papilla. One day after UUO, there were no visible pathologic changes. However, the day 7 sample exhibited morphologic changes manifested by proximal tubule dilation (*), tubular atrophy (arrows) and extracellular matrix (ECM) accumulation (○). After 14 days, the kidney no longer had a normal structure, with collapsed tubules and increased interstitial spaces containing mononuclear and interstitial cells (○). Scale bars represent 200 μm.

athy as well as mechanisms responsible for progressive renal fibrosis.⁶ There are many quantifiable pathophysiologic features of the UO model that occur within 1 week of the onset of ureteral ligation that make this an increasingly good experimental model for study. Most reported evidence suggests that the rodent model of UO is reflective of the human renal disease process.⁷

In the clinical setting, the major modalities for evaluating the mechanisms of obstructive uropathy include ultrasonography, nuclear scintigraphy, and CT. Computed tomography can be used to assess the urinary system for different purposes, and the most important advantage of CT is that it can be employed to visualize the entire urinary system simultaneously. This modality also provides accurate information regarding the detailed anatomy and vasculature of the kidneys.⁸ Micro-CT was developed as an experimental tool for imaging diverse mineralized animal tissues, and the enhancement provided by the contrast agent yields sufficient intra-organ contrast to detect soft organs.²

In the current study, we initially performed contrast-enhanced micro-CT to acquire detailed anatomic and morphologic data in a mouse model of UO. Using noninvasive imaging, we were able to follow renal lesions using micro-CT for 2 weeks and successfully established the morphology and function of the kidneys. With respect to serial imaging, micro-CT has the advantages of not requiring that the animals be sacrificed and providing data for the entire urinary tract simultaneously.

A few previous studies have assessed the kidney anatomy and function in mice.⁹ In addition, Almajdub *et al*¹⁰ regards mouse kidney phenotyping as being an important issue, and *in vivo* imaging allows for longitudinal studies. Therefore, micro-CT appears to be a suitable method for phenotyping the kidney anatomy. The above authors also demonstrate the accuracy of *in vivo* micro-CT in quantifying the kidney volume and distinguishing anatomic differences between mouse strains. Similar findings have been reported in large animals.¹¹

Renal pelvis dilatation may be caused by various disorders. Congenital urinary tract obstruction is the most important identifiable cause of renal failure in infants and children,¹² and the measurements of the renal length and parenchymal thickness are clinically relevant for assessing the renal function. Obtaining an accurate kidney size is of value for monitoring the disease progress. In the current study, the histologic results supported the imaging results.

In the clinical setting, Mohamed *et al* used contrast-enhanced spiral CT to determine the glomerular filtration rate (GFR) in patients with chronic obstructive uropathy.¹³ However, we consider it appropriate to estimate the renal function by measuring the renal length or parenchymal thickness and engorgement/excretion time, as the GFR may be falsely high if the measurement depends only on calculating the level of total enhancement.

Other previous studies have shown that high spatial resolution 3-dimensional anatomic and functional mouse kidney images may be obtained without contrast agent on high-field MRI.^{9,14} Another study compared the efficacy of contrast-enhanced micro-CT and MRI in animal models. The authors concluded that, in addition to the advantages of not exposing the animal to ionizing radiation, MRI provides a more complete assessment.¹⁵ In contrast, micro-CT imaging can be performed easily and also allows for functional studies, while also being readily implemented in animal facilities.

In previously reported studies, the renal length and volume were measured to evaluate the presence or severity of renal insufficiency, in which the degree of kidney atrophy paralleled the extent of deterioration of the renal function.^{16,17} In the present study, the renal coronal length and axial thickness on the UO side did not change markedly during the UO period, while the renal coronal parenchymal thickness was found to decrease over time on the UO side after 7 days. This observation indicates that the hydronephrosis induced atrophic reduction of the amount of kidney tissue.

Complete UO involves a rapid sequence of changes within 24 hours, leading to hydronephrosis and reduced glomerular filtration.⁶ Progression to severely hydronephrotic kidneys with noticeable loss of the renal parenchyma occurs after just 1 week, as demonstrated above. However, clinically obstructive nephropathy involves partial obstruction and recanalization, rather than complete obstruction, and various models of partial UO and ureteral obstruction reversal have been developed.¹⁸⁻²⁰ We are planning to perform further experiments to evaluate the characteristics of partial UO and potential for reversal of ureteral obstruction.

One limitation of the present study is that there was no evidence of findings specific for renal fibrosis. However, the use of a combination of other noninvasive tests, such as diffusion-weighted imaging,²¹ is expected to enable the clinician to identify renal fibrosis.

In conclusion, the present study demonstrated that microcomputed tomography is a useful tool for noninvasively evaluating the renal structure and function *in vivo* in a mouse model of UO. The current results indicate that micro-CT is useful for conducting further experimental research using small animals.

Acknowledgments

Jiangang Hou and Masayuki Fujino contributed equally in this work. This study was supported by research grants from the Ministry of Education, Culture, Sports, Science and Technology of Japan (Grants-in-Aid 20390349, 21659310) and the National Center for Child Health and Development (22-10, 24-1:756). All authors have no conflicts of interest to declare.

References

- Klahr S, Morrissey JJ. The role of growth factors, cytokines, and vasoactive compounds in obstructive nephropathy. *Semin Nephrol* 1998;**18**(6):622–632
- Neues F, Epple M. X-ray microcomputer tomography for the study of biomineralized endo- and exoskeletons of animals. *Chem Rev* 2008;**108**(11):4734–4741
- Kuratsune M, Masaki T, Hirai T, Kiribayashi K, Yokoyama Y, Arakawa T *et al.* Signal transducer and activator of transcription 3 involvement in the development of renal interstitial fibrosis after unilateral ureteral obstruction. *Nephrology (Carlton)* 2007;**12**(6):565–571
- Hou J, Cai S, Kitajima Y, Fujino M, Ito H, Takahashi K *et al.* 5-Aminolevulinic acid combined with ferrous iron induces carbon monoxide generation in mouse kidneys and protects from renal ischemia-reperfusion injury. *Am J Physiol Renal Physiol* 2013;**305**(8):F1149–1157
- Fujino M, Li XK, Kitazawa Y, Funeshima N, Guo L, Okuyama T *et al.* Selective repopulation of mice liver after Fas-resistant hepatocyte transplantation. *Cell Transplant* 2001;**10**(4-5):353–361
- Vaughan ED Jr, Marion D, Poppas DP, Felsen D. Pathophysiology of unilateral ureteral obstruction: studies from Charlottesville to New York. *J Urol* 2004;**172**(6 Pt 2):2563–2569
- Klahr S, Morrissey J. Obstructive nephropathy and renal fibrosis. *Am J Physiol Renal Physiol* 2002;**283**(5):F861–875
- Young SW, Noon MA, Marincek B. Dynamic computed tomography time–density study of normal human tissue after intravenous contrast administration. *Invest Radiol* 1981;**16**(1):36–39
- Wallace DP, Hou YP, Huang ZL, Nivens E, Savinkova L, Yamaguchi T *et al.* Tracking kidney volume in mice with polycystic kidney disease by magnetic resonance imaging. *Kidney Int* 2008;**73**(6):778–781
- Almajdub M, Magnier L, Juillard L, Janier M. Kidney volume quantification using contrast-enhanced *in vivo* X-ray micro-CT in mice. *Contrast Media Mol Imaging* 2008;**3**(3):120–126
- Sommer G, Bouley D, Frisoli J, Pierce L, Sandner-Porkristl D, Fahrig R. Determination of 3-dimensional zonal renal volumes using contrast-enhanced computed tomography. *J Comput Assist Tomogr* 2007;**31**(2):209–213
- Seikaly MG, Ho PL, Emmett L, Fine RN, Tejani A. Chronic renal insufficiency in children: the 2001 Annual Report of the NAPRTCS. *Pediatr Nephrol* 2003;**18**(8):796–804
- El-Ghar ME, Shokeir AA, El-Diasty TA, Refaie HF, Gad HM, El-Dein AB. Contrast enhanced spiral computerized tomography in patients with chronic obstructive uropathy and normal serum creatinine: a single session for anatomical and functional assessment. *J Urol* 2004;**172**(3):985–988
- Cheong B, Muthupillai R, Rubin MF, Flamm SD. Normal values for renal length and volume as measured by magnetic resonance imaging. *Clin J Am Soc Nephrol* 2007;**2**(1):38–45
- Martiniova L, Kotys MS, Thomasson D, Schimel D, Lai EW, Bernardo M *et al.* Noninvasive monitoring of a murine model of metastatic pheochromocytoma: a comparison of contrast-enhanced microCT and nonenhanced MRI. *J Magn Reson Imaging* 2009;**29**(3):685–691
- Khati NJ, Hill MC, Kimmel PL. The role of ultrasound in renal insufficiency: the essentials. *Ultrasound Q* 2005;**21**(4):227–244
- Widjaja E, Oxtoby JW, Hale TL, Jones PW, Harden PN, McCall IW. Ultrasound measured renal length versus low dose CT volume in predicting single kidney glomerular filtration rate. *Br J Radiol* 2004;**77**(921):759–764
- Thornhill BA, Burt LE, Chen C, Forbes MS, Chevalier RL. Variable chronic partial ureteral obstruction in the neonatal rat: a new model of ureteropelvic junction obstruction. *Kidney Int* 2005;**67**(1):42–52
- Thornhill BA, Forbes MS, Marcinko ES, Chevalier RL. Glomerulotubular disconnection in neonatal mice after relief of partial ureteral obstruction. *Kidney Int* 2007;**72**(9):1103–1112
- Cochrane AL, Kett MM, Samuel CS, Campanale NV, Anderson WP, Hume DA *et al.* Renal structural and functional repair in a mouse model of reversal of ureteral obstruction. *J Am Soc Nephrol* 2005;**16**(12):3623–3630
- Wittsack HJ, Lanzman RS, Mathys C, Janssen H, Modder U, Blondin D. Statistical evaluation of diffusion-weighted imaging of the human kidney. *Magn Reson Med* 2010;**64**(2):616–622

© 2015 Hou et al.; licensee The International College of Surgeons. This is an Open Access article distributed under the terms of the Creative Commons Attribution Non-commercial License which permits use, distribution, and reproduction in any medium, provided the original work is properly cited, the use is non-commercial and is otherwise in compliance with the license. See: <http://creativecommons.org/licenses/by-nc/3.0>